Mixing of Longitudinal and Transverse Dynamics in Liquid Water

M. Sampoli,[1] G. Ruocco,[2] and F. Sette[3]
[1]*Universitá di Firenze and Istituto Nazionale di Fisica della Materia, I-50139, Firenze, Italy*
[2]*Universitá di L'Aquila and Istituto Nazionale di Fisica della Materia, I-67100, L'Aquila, Italy*
[3]*European Synchrotron Radiation Facility, B.P. 220 F-38043 Grenoble Cedex, France*
(Received 13 March 1997)

Molecular dynamics simulations of liquid water in the 1.3–35 nm^{-1} momentum transfer (Q) region show two excitations with a Q dependent symmetry character. The symmetry analysis suggests that the observed anomalies in the high frequency collective dynamics originate from relaxation processes responsible for (i) the appearance of a propagating transverse dynamics at high frequency, (ii) the transition from normal to *fast* sound, and (iii) a mixed symmetry of the two modes at large Q. [S0031-9007(97)03759-9]

PACS numbers: 61.20.Ja, 61.20.Lc, 61.25.Em

The investigation of large wave vector excitations in liquid water has been a challenging task since the pioneering computational [1] and experimental [2] studies on its dynamic structure factor, $S(Q, \omega)$. These works revealed the existence of acoustic-like excitations propagating with a speed, $v_\infty = 3300$ m/s, corresponding to a value more than twice the hydrodynamic sound ($v_o \approx 1500$ m/s). Subsequent works studied this issue by molecular dynamics (MD) [3,4], inelastic neutron-(INS) [5], and inelastic x-ray scattering (IXS) [6,7]. The high frequency picture emerging from $S(Q, \omega)$ of H_2O can be summarized as follows: (i) The acousticlike mode propagates with v_∞ in the 4 to 14 nm^{-1} Q range. (ii) For Q larger than 4 nm^{-1}, there is a second, weakly dispersing mode with an energy of $\approx$5 meV. (iii) Both modes involve the motion of the molecular center of mass. (iv) At $Q = 4$ nm^{-1}, the energy of the two modes becomes comparable, and in the 1 to 4 nm^{-1} Q region only one mode is observed; the sound velocity of this mode changes, decreasing Q, from v_∞ toward v_o. This picture indicates the existence of two branches, one strongly dispersing and the other weakly dispersing with Q. The first one is identified as the sound branch with a bend up in the region below $Q = 4$ nm^{-1}. The second one, on the basis of MD simulations [1,4] and of INS and IXS results on ice crystals [7,8], can be related to a localized motion reminiscent of the transverse dynamics in the crystal, and to the bending motion between three hydrogen-bonded water molecules. The most important point, however, is not yet settled: is the physical mechanism responsible for the bending of the sound branch and for the observation of a second mode at Q larger than 4 nm^{-1} a feature common to a large class of liquids or is it specific to water?

In this Letter we report a numerical MD investigation on the symmetry character of the modes observed in liquid water. The MD results in the Q range of the IXS and INS experiments show the existence of two different dynamic regimes. In the small Q limit, $Q < 2$ nm^{-1}, the dynamics is liquidlike; there are pure longitudinal modes propagating with $v = v_o$, and the transverse dynamics is relaxationallike. In the opposite limit, at Q larger than 4 nm^{-1}, the dynamics is solidlike; there are two modes with energies close to the longitudinal and transverse phonon branches in ice. Here, however, contrary to ice, both modes have a large mixing of longitudinal and transverse symmetry. A propagating transverse dynamics starts to appear in the same intermediate Q region where the longitudinal branch acquires a transverse component, and its sound velocity changes from v_o to v_∞. The transition between the two regimes is found in the Q-ω region, corresponding to the length scale and lifetime of local order in liquid water. Therefore, these results link the anomalies in the high frequency collective dynamics of liquid water to relaxation processes originating from locally ordered molecular assemblies.

The MD simulation was carried out considering $N = 4000$ "D_2O" SPC/E [9] molecules enclosed in a cubic box with periodic boundary conditions [10]. The molar volume was 18 cm^3 and the temperature $\approx$250 K, i.e., the temperature of maximum density for the SPC/E potential model [11]. The electrostatic long-range interactions are taken into account with the tapered reaction field method, and the rotational equations of motion were integrated using an improved algorithm [12]. After thermalization, the molecular trajectories have been followed by about 100 ps and stored every 10 fs, i.e., every five integration time steps. From the stored configurations, we have evaluated the instantaneous $\mathbf{Q}$ component of the density fluctuations of the center of mass $\rho_{\mathbf{Q}}(t)$:

$$\rho_{\mathbf{Q}}(t) = 1/\sqrt{N} \sum_j \exp[i\mathbf{Q} \cdot \mathbf{R}_j(t)],$$

where $\mathbf{R}_j(t)$ is the instantaneous position of the molecular center of mass [13]. The dynamic structure factor is calculated from the power spectrum of $\rho_{\mathbf{Q}}(t)$, i.e., $S(\mathbf{Q}, \omega) = |\mathcal{FT}\{\rho_{\mathbf{Q}}(t)\}|^2$. To reduce the noise in $S(\mathbf{Q}, \omega)$, the Welsh method [15] with a Hanning window has been employed.

The time window was $\Delta t \approx 20$ ps, giving rise to an energy resolution of 0.04 meV. The $S(\mathbf{Q}, \omega)$ has been averaged over independent directions of $\mathbf{Q} = \frac{2\pi}{L}(h, k, l)$

 0031-9007/97/79(9)/1678(4)$10.00

(where $L = 4.93$ nm is the box length) at several Q values in the 1.3 to 35 nm^{-1} range. The longitudinal current spectra, $C_L(Q,\omega)$, are obtained as $C_L(Q,\omega) = \omega^2 S(Q,\omega)/Q^2$.

The comparison between the calculated $S(Q,\omega)$ and the inelastic x-ray scattering data measured at 278 K [6] is very good for any of the Q values used in the IXS experiment. As a consequence of the capability of the present potential model to represent well the dynamics of real water at normal density, we expect that also the transverse dynamics, a quantity not experimentally accessible, can be reliably determined from the MD data. We therefore calculated the transverse current spectra $C_T(\mathbf{Q},\omega) = |\mathcal{FT}\{\mathbf{j}^T_{\mathbf{Q}}(t)\}|^2$ with

$$\mathbf{j}^T_{\mathbf{Q}}(t) = 1/\sqrt{N}\sum_j [\hat{\mathbf{Q}} \times \{\hat{\mathbf{Q}} \times \mathbf{v}_j(t)\}] \exp[i\mathbf{Q}\cdot\mathbf{R}_j(t)] .$$

In Fig. 1 we report examples of longitudinal [Figs. 1(a) and 1(b)] and transverse [Figs. 1(c) and 1(d)] current spectra at selected Q values. Both $C_L(Q,\omega)$ and $C_T(Q,\omega)$, show the existence of two excitations. The high frequency excitation disperses with Q, and its sound velocity changes from $\approx$2000 m/s to $\approx$3300 m/s. This excitation appears at each Q value in the longitudinal current spectra, while it is found in the transverse current spectra only at $Q > 4$ nm^{-1}. We assign this feature to a quasilongitudinal sound branch, and we call it L mode for its longitudinal character in the $Q \to 0$ limit. The behavior of the low frequency excitation is in some sense opposite; it is always present in the transverse current spectra, while it appears in the longitudinal current spectra only at $Q > 4$ nm^{-1}. This low frequency feature is from now on referred to as the T mode. At small Q, the T mode disperses with a sound velocity of $\approx$1500 m/s and becomes almost nondispersing at $Q > 7$ nm^{-1}.

The calculated spectra have been fitted with simple models to summarize the excitations in terms of their energy [$\Omega_\eta(Q)$, $\eta = \{L,T\}$, i.e., the position of the current spectra maxima], their energy width [$\Gamma_\eta(Q)$], and their integrated intensity [$I_\eta(Q)$]. Different line shapes have been used, ranging from a simple damped harmonic oscillator (DHO) [16] to more refined viscoelastic models [17]. It is beyond the aim of the present work to discuss the physical meaning and the reliability of the different approaches. All these models, however, give fitting parameters which are consistent among each other within their uncertainties, and we report here the parameters obtained using the DHO line shape for the T mode and the viscoelastic theory with an exponential memory function for the L mode. The corresponding best fits to the MD data are shown in Figs. 1(a)–1(d).

The values of the excitation energies, $\Omega_L(Q)$ and $\Omega_T(Q)$, are reported in Fig. 2. Figure 2(a) shows the complete investigated Q region. The dispersion relation of the L modes follows the universal behavior of liquid systems; i.e., a minimum appear at about the Q value where the $S(Q)$ attains its maximum. A similar minimum, although less pronounced, is found in the T modes branch. Figures 2(b) and 2(c) show the small momentum transfer region in an expanded Q scale. In Fig. 2(c) the change in slope of the L branch marks the transition between v_o and v_∞.

The MD results agree well with available INS and IXS data on liquid water, and they can be directly compared with measurements and lattice dynamics calculations of solid water in its ice *Ih* form [7,8]. In ice crystals, as in the liquid, there are two phonon modes with energies below $\approx$30 meV [18]. These are the longitudinal and transverse phonon branches, linearly dispersing at small Q with velocities $v = 4000$ m/s and $v \approx 2000$ m/s, respectively. Moreover, the transverse branch becomes almost flat at Q larger than 7 nm^{-1}. Therefore, the MD results not only confirm that at Q larger than 4 nm^{-1} the longitudinal dynamics in liquid water become similar to that of the crystalline solid, but also show that the transverse dynamics acquires a solidlike behavior in about the same Q region. There is, however, an important difference between liquid and solid in the symmetry character of the two branches. In the solid, a dominant longitudinal or transverse character is preserved throughout the considered Q region. In the liquid, the MD results show that, as a consequence of lack of translational invariance, the pure symmetry character of the two modes is rapidly lost, and at large Q both modes contribute in similar amounts to $C_L(Q,\omega)$ and $C_T(Q,\omega)$.

The MD results obtained at low Q, i.e., below 2 nm^{-1}, can be compared with both experiment and common wisdom for the collective dynamics of simple liquids in the $Q \to 0$ limit; i.e., only one mode survives in each current spectrum. In $C_L(Q,\omega)$, the L mode propagates with a velocity of sound approaching the hydrodynamic value measured in the macroscopic time- and length-scale limits. In $C_T(Q,\omega)$, the T mode loses its propagating character observed in the 2–4 nm^{-1} region, and one could infer that the transverse dynamics becomes progressively relaxational from the pileup of spectral intensity toward zero frequency. The transition of the L mode to a pure longitudinal symmetry propagating with the v_o, and the disappearance of the T mode, bring the collective dynamics of liquid water back to the behavior expected for a simple liquid in the macroscopic limit.

The transition from the low frequency and low Q hydrodynamic behavior to the high frequency solidlike regime has already been observed in many glass-forming liquids [19]. This transition takes place at a Q value where the pulsation of the sound wave ω equals the inverse of the structural relaxation time τ. Manifestations of this transition, among other phenomena, are (i) the increase of the longitudinal sound velocity from v_o toward v_∞, and (ii) the appearance of a propagating transverse dynamics. This behavior is very similar to the one found here for liquid water, as shown by the Q dependence of the parameters reported in Fig. 2, which can be scaled to the typical α-relaxation process [19]. At variance with other known glass-forming systems, where the condition $\omega\tau = 1$ is

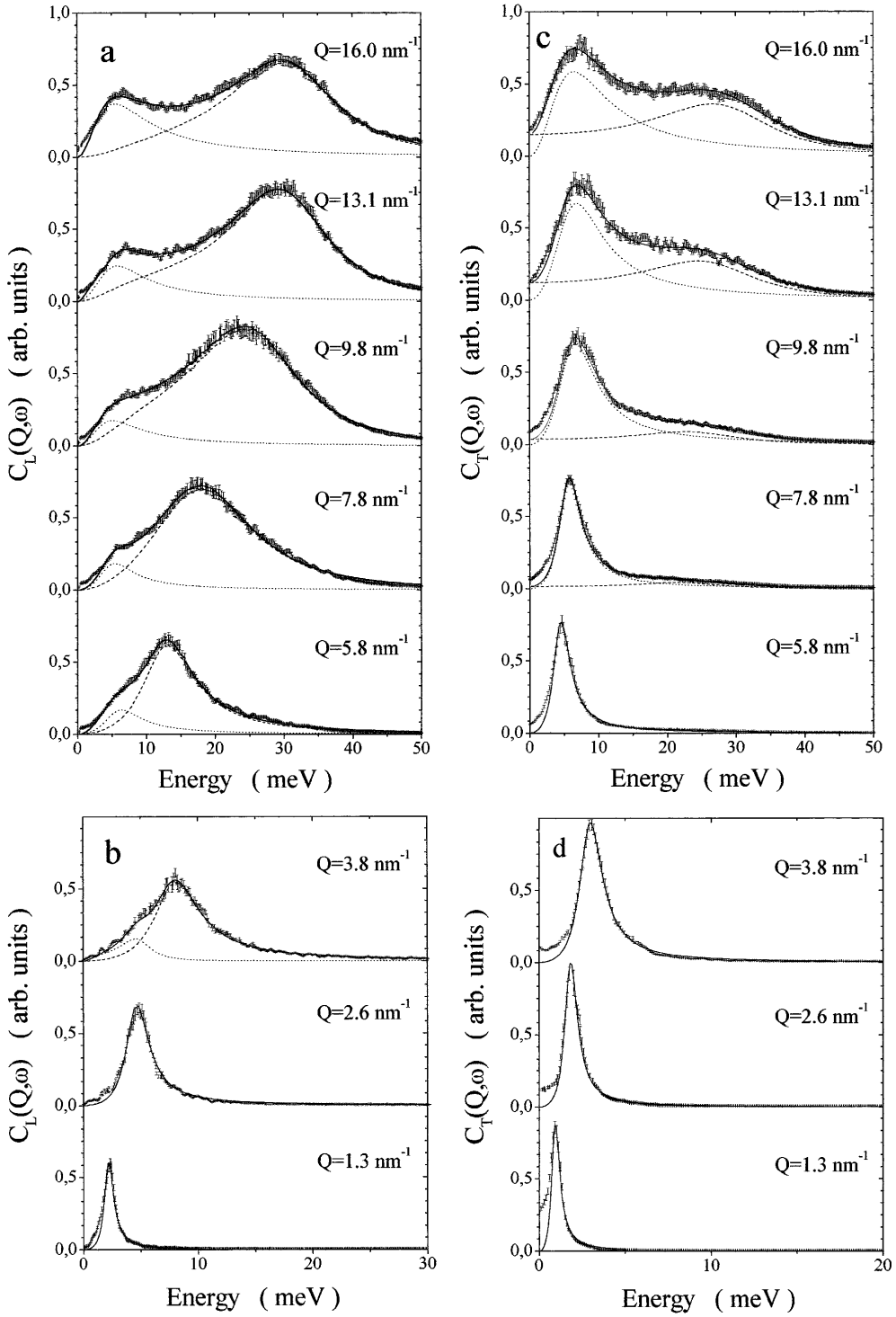

FIG. 1. The longitudinal (a),(b) and transverse (c),(d) current spectra are reported with the error bars at the indicated Q values. The full lines are the best fits to the spectra as indicated in the text. Dashed (dotted) line is the individual contribution to the fit coming from the L mode (T mode).

fulfilled at frequencies below 10^{10} Hz, in water the transition is found at much higher frequencies, $\approx 2.5 \times 10^{11}$ Hz, i.e., $\tau \approx 0.6$ ps. Finally, the wavelength marking the transition, $\lambda_\tau = 2\pi v_o \tau \approx 3$ nm, is comparable to the structural correlation length derived from $S(Q)$ measurements by Bosio *et al.* [20]. This indicates that the origin of the transition between the two dynamic regimes, besides from dynamic relaxational processes, may also come from the local structural order existing in liquid water. A temperature study would discriminate between the dynamic and structural effects.

In conclusion, the analysis of the longitudinal and transverse current spectra calculated by MD simulations, of liquid water shows that the dynamics can be described within

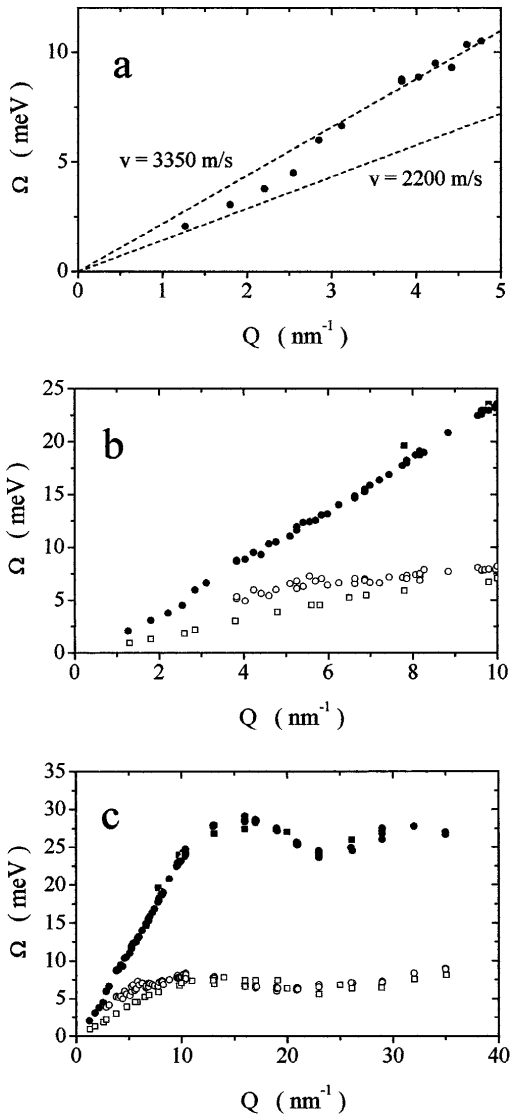

FIG. 2. Energy position of the L modes (full symbols) and T modes (open symbols) in three different Q regions: (a) $Q = 0-5$ nm^{-1}; (b) $Q = 0-10$ nm^{-1}, (c) $Q = 0-40$ nm^{-1}. The circles [squares] represent the $\Omega_\eta(Q)$ parameter obtained from the $C_L(Q,\omega)$ [$C_T(Q,\omega)$]. The slopes of the lines in (a) correspond to the longitudinal v_o and v_∞ obtained for the present potential model.

the same framework used for other molecular liquids. In particular, it is possible to derive a characteristic time scale where the density fluctuations change from the macroscopic to a solidlike elastic behavior. Here the system has an increased sound velocity and supports transverse excitations. Differently from most other liquids, the value of τ is an order of magnitude smaller in liquid water. Speculatively, this can be linked to the light mass of H_2O, and therefore the relaxation process would be strongly associated to the single particle motion, in spite of the strong local tetrahedral order known to exist on average.

[1] A. Rahman and F. H. Stillinger, Phys. Rev. A **10**, 368 (1974).
[2] J. Teixeira, M. C. Bellissent-Funel, S. H. Chen, and B. Dorner, Phys. Rev. Lett. **54**, 2681 (1985).
[3] R. W. Impey, P. A. Madden, and I. R. McDonald, Mol. Phys. **46**, 513 (1982); M. Wojcik and E. Clementi, J. Chem. Phys. **85**, 6085 (1986); M. A. Ricci, D. Rocca, G. Ruocco, and R. Vallauri, Phys. Rev. Lett. **61**, 1958 (1988); Phys. Rev. A **40**, 7226 (1989); U. Balucani *et al.*, Phys. Rev. E **47**, 1677 (1993); U. Balucani, G. Ruocco, M. Sampoli, A. Torcini, and R. Vallauri, Chem. Phys. Lett. **209**, 408 (1993); F. Sciortino and S. Sastry, J. Chem. Phys. **100**, 3881 (1994); U. Balucani, J. P. Brodholt, and R. Vallauri, J. Phys. C **8**, 9269 (1997); V. Tozzini and M. P. Tosi, Phys. Chem. Liq. **33**, 191 (1996).
[4] S. Sastry, F. Sciortino, and E. Stanley, J. Chem. Phys. **95**, 7775 (1991).
[5] P. Bosi, F. Dupré, F. Menzinger, F. Sacchetti, and M. C. Spinelli, Il Nuovo Cimento Lett. **21**, 436 (1978); F. J. Bermejo, M. Alvarez, S. M. Bennington, and R. Vallauri, Phys. Rev. E **51**, 2250 (1995).
[6] F. Sette *et al.*, Phys. Rev. Lett. **75**, 850 (1995); F. Sette *et al.*, Phys. Rev. Lett. **77**, 83 (1996).
[7] G. Ruocco *et al.*, Nature (London) **379**, 521 (1996); G. Ruocco *et al.*, Phys. Rev. B **54**, 14 892 (1996).
[8] B. Renker, Phys. Lett. **30A**, 493 (1969).
[9] H. J. C. Berendsen, J. P. M. Postma, W. F. Van Gunsteren, and H. J. Hermans, in *Intermolecular Forces*, edited by B. Pulmann (Reidel, Dordrecht, 1981), p. 331.
[10] The "D_2O" molecules have been preferred to "H_2O" for their higher momenta of inertia, enabling longer integration time steps of the equation of motion in the microcanonical ensemble.
[11] P. H. Poole, F. Sciortino, U. Essmann, and H. E. Stanley, Phys. Rev. E **48**, 3799 (1993).
[12] G. Ruocco and M. Sampoli Mol. Phys. **82**, 875 (1994); Mol. Sim. **15**, 281 (1995).
[13] In this simulation we discuss the center of mass dynamics and not the orientational dynamics, mainly related to the hydrogen current spectra (e.g., see Ref. [14]).
[14] D. Bertolini and A. Tani, Mol. Phys. **75**, 1047 (1992).
[15] P. D. Welsh, IEEE Trans. Audio Electroacoust. **AU15**, 70 (1967); M. H. Hayes, *Statistical Digital Signal Processing and Modelling* (John Wiley, London, 1996).
[16] B. Fak and B. Dorner, Institute Laue Langevin (Grenoble, France), technical report No. 92FA008S (1992).
[17] U. Balucani and M. Zoppi, *Dynamics of the Liquid State* (Clarendon Press, Oxford, 1994).
[18] The comparison between the dispersion relations in liquid and solid water are done considering: (i) an orientational averaging in the ice Brillouin zone, and (ii) the extended Brilouin zone scheme, appropriate for the strong local tetrahedral symmetry existing in ice.
[19] See *Dynamics of Disordered Materials II*, edited by A. J. Dianoux, W. Petry, and D. Richter (North-Holland, Amsterdam, 1993).
[20] L. Bosio, J. Teixeira, and H. E. Stanley, Phys. Rev. Lett. **46**, 597 (1981).